Course Outline

1. Symmetry, Group Theory, and Electronic Structure

2. Ground State Spectroscopic Methods

3. Excited State Spectroscopic Methods

3.1 Valence Electronic Spectroscopy

3.2 Core Electronic Spectroscopy

Core Level Spectroscopy

- probe deeper binding energy electron
- e^- not directly involved in bonding
  - radial distribution of atomic orbitals is too small to allow for good overlap
- three types of processes expected
  - photoionisation → XPS, EXAFS
  - bound state excitation → XANES
  - photoionisation + relaxation
    - X-ray photoemission → XES
    - Auger electron emission → AES
- each provides different information

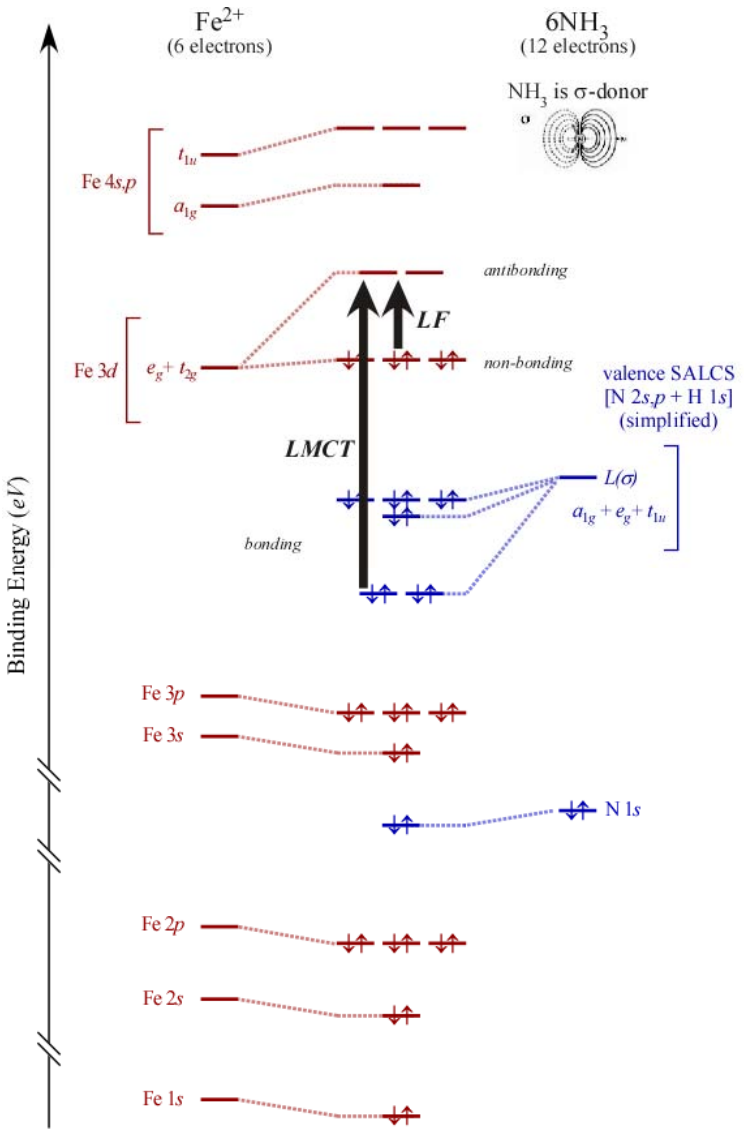

Relaxation Processes in X-ray Photoexcitation Processes

- Two basic mechanisms (like regular spectroscopy)
- Radiative (photoemission/fluorescence)
  - can be extremely informative
  - dominates at higher *Z*
  - more efficient in *K*-shell decay
- Non-radiative (electron ejection)
  - Auger decay (dominant at low *Z*)
  - Coster-Kronig decay
- measurements of 'absorption' are often made using secondary decay
  - fluorescence yield measurements
  - electron yield measurements

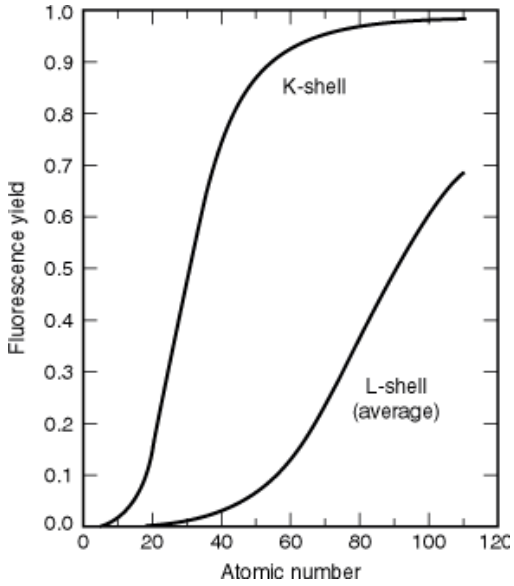

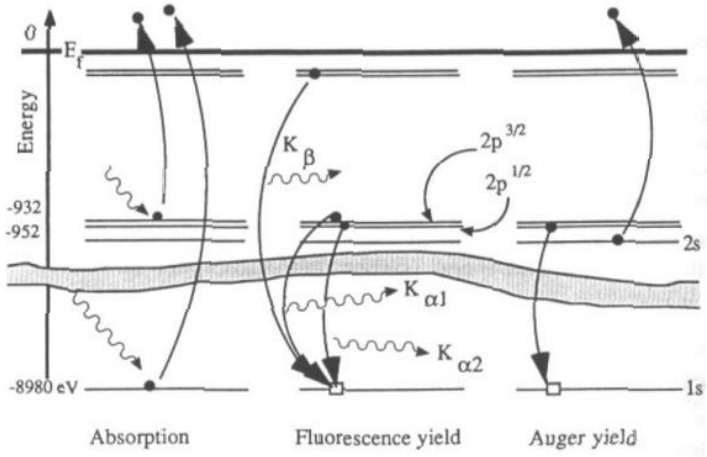

Nomenclature for X-ray Spectroscopy → living with history...

- still use old physics terminology... $Shell_{Line\#}$
  - use first atomic quantum number labels: *K* = 1, *L* = 2, *M* = 3, *etc.*
  - line number simply by energy ordering of different components
    - higher energy = lower number
- *very important* - more absorption lines than orbitals...
  - excited state Spin-Orbit Coupling!
  - *e.g.* 2*p* splits into $2p_{1/2}$ and $2p_{3/2}$

$$\begin{cases} L = 1 \\ S = \frac{1}{2} \end{cases} \rightarrow J = \frac{3}{2}, \frac{1}{2}$$

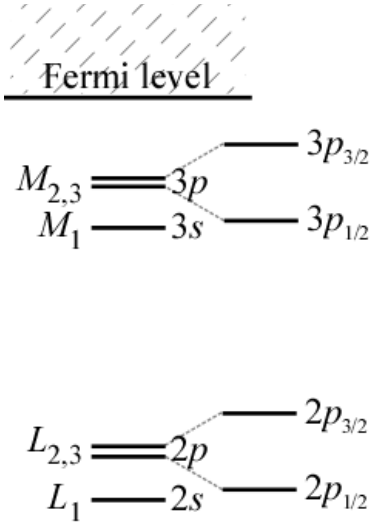

- for secondary processes, additional information is given based on what happens next:
  - XES → second labels are given α_i, β_i numbering based on origin of decay
  - AES → three labels describing origin of each electron involved...

3.2 Core Level Electronic Spectroscopy

XES

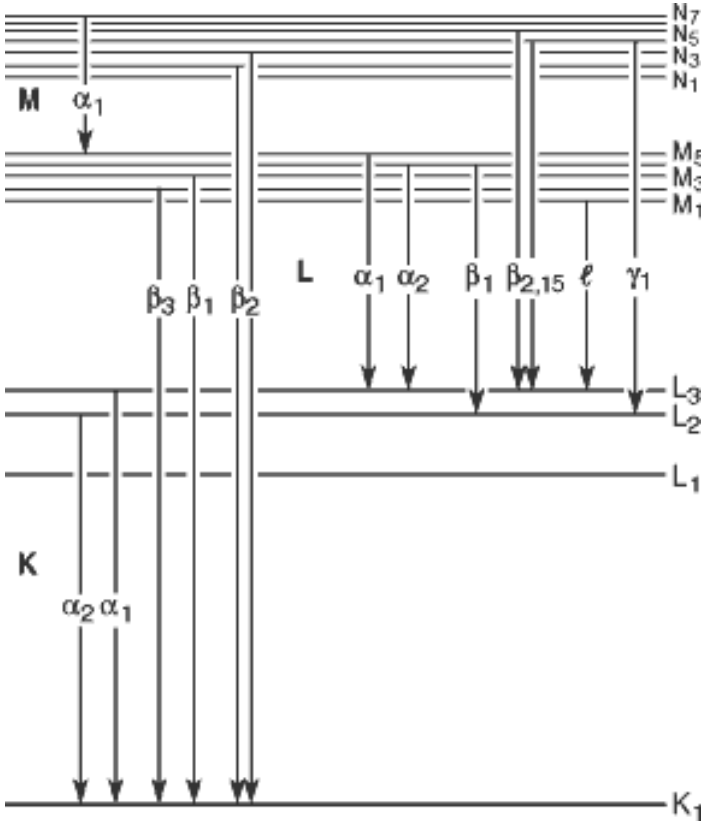

AES

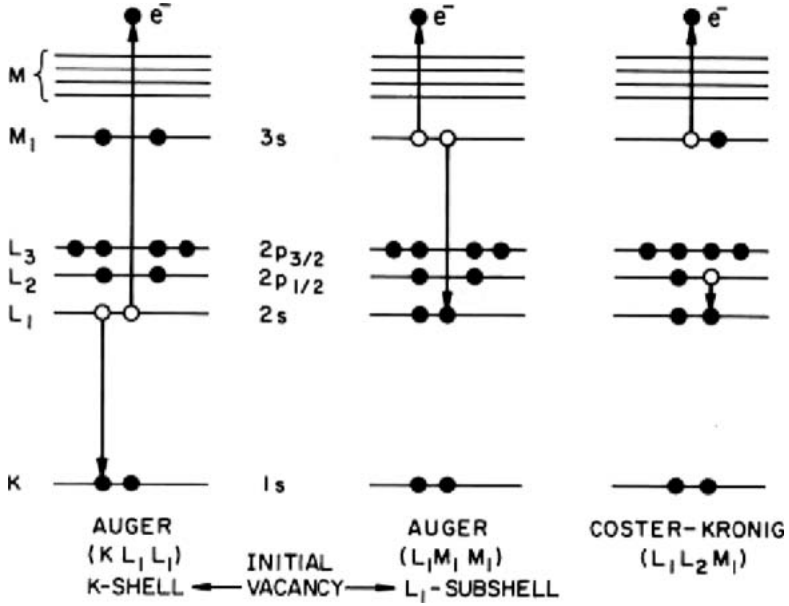

X-ray Photoelectron Spectroscopy (XPS)

- *aka* ESCA (electron spectroscopy for chemical analysis)
  - binding energies are distinct for specific core orbitals – element specific!
  - often used for elemental analysis of complex systems
- ionisation of core "atomic" levels
  - core electrons are perturbed through shielding/deshielding
  - binding energy is obtained from Einstein equation: $E_k = h\nu - E_b$
  - shift in binding energy from 'reference' give *chemical shift*
- core binding energies unique for each element
  - generally assume that binding energy is energy of atomic orbital in initial species → *Koopmans' theorem*
    - no change in electronic structure due to ionisation
    - this is never really true – but generally not bad

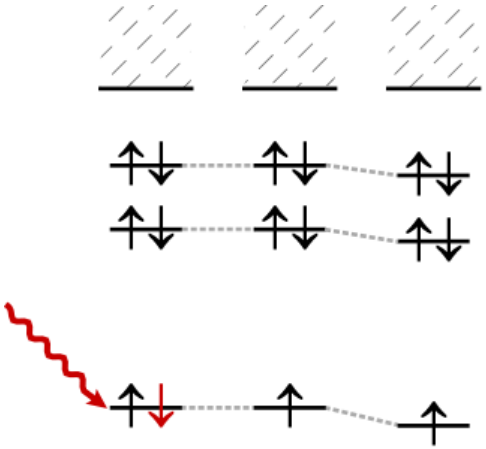

Selected Electron Binding Energies

Element	K 1s	L_1 2s	L_2 $2p_{1/2}$	L_3 $2p_{3/2}$	M_1 3s	M_2 $3p_{1/2}$	M_3 $3p_{3/2}$
1 H	13.6						
2 He	24.6*						
3 Li	54.7*						
4 Be	111.5*						
5 B	188*						
6 C	284.2*						
7 N	409.9*	37.3*					
8 O	543.1*	41.6*					
9 F	696.7*						
10 Ne	870.2*	48.5*	21.7*	21.6*			
11 Na	1070.8†	63.5†	30.65	30.81			
12 Mg	1303.0†	88.7	49.78	49.50			
13 Al	1559.6	117.8	72.95	72.55			
14 Si	1839	149.7*b	99.82	99.42			
15 P	2145.5	189*	136*	135*			
16 S	2472	230.9	163.6*	162.5*			
17 Cl	2822.4	270*	202*	200*			
18 Ar	3205.9*	326.3*	250.6†	248.4*	29.3*	15.9*	15.7*
19 K	3608.4*	378.6*	297.3*	294.6*	34.8*	18.3*	18.3*
20 Ca	4038.5*	438.4†	349.7†	346.2†	44.3 †	25.4†	25.4†
21 Sc	4492	498.0*	403.6*	398.7*	51.1*	28.3*	28.3*
22 Ti	4966	560.9†	460.2†	453.8†	58.7†	32.6†	32.6†

3.2.1 X-ray Photoelectron Spectroscopy (XPS)

- Effect of Excited State Spin Orbit Coupling…
  - splits transitions from orbitals that carry orbital angular momentum (*p*,*d*,*f*)
  - relative intensity of peaks depends on *J*-degeneracy (2*J*+1)

$$\left.\begin{matrix} L=0 \\ S=\frac{1}{2} \end{matrix}\right\rangle J=\frac{1}{2}$$

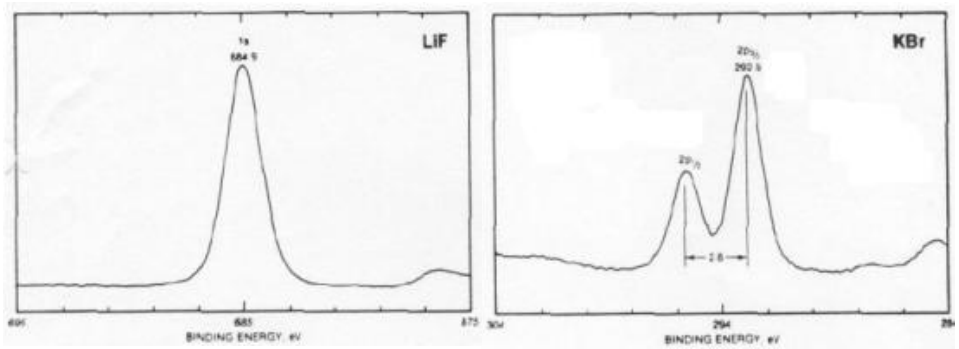

$$\left.\begin{matrix} L=1 \\ S=\frac{1}{2} \end{matrix}\right\rangle S=\frac{3}{2},(4)\quad S=\frac{1}{2},(2)$$

$$\left.\begin{matrix} L=2 \\ S=\frac{1}{2} \end{matrix}\right\rangle S=\frac{5}{2},(6)\quad S=\frac{3}{2},(4)$$

$$\left.\begin{matrix} L=3 \\ S=\frac{1}{2} \end{matrix}\right\rangle S=\frac{7}{2},(8)\quad S=\frac{5}{2},(6)$$

- magnitude of SOC changes little – function of atomic orbitals not molecular species
  - some (generally small) effect from effective charge on atom and chemical shielding

Core Level Chemical Shifts

- directly related to effective nuclear charge (Z_{eff}) on atom
  - chemical shifts can be correlated with *oxidation state* of atom

$$\uparrow Z_{eff} \equiv \uparrow E_b$$

higher positive charge on atom increases energy required to remove electron

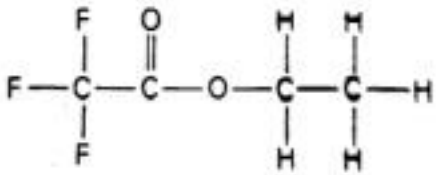

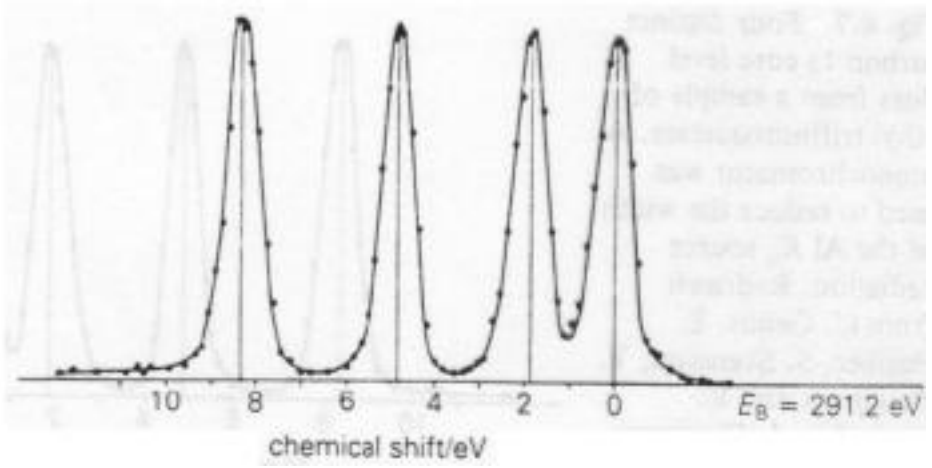

Fig. 6.7 Four distinct carbon 1*s* core level lines from a sample of ethyl trifluoroacetate. A monochromator was used to reduce the width of the Al K_α source radiation. Redrawn from U. Gelius, E. Basilier, S. Svensson, T. Bergmark and K. Siegbahn, *J. Electronic Spectr.*, **2**, 405 (1974).

3.2.1 X-ray Photoelectron Spectroscopy (XPS)

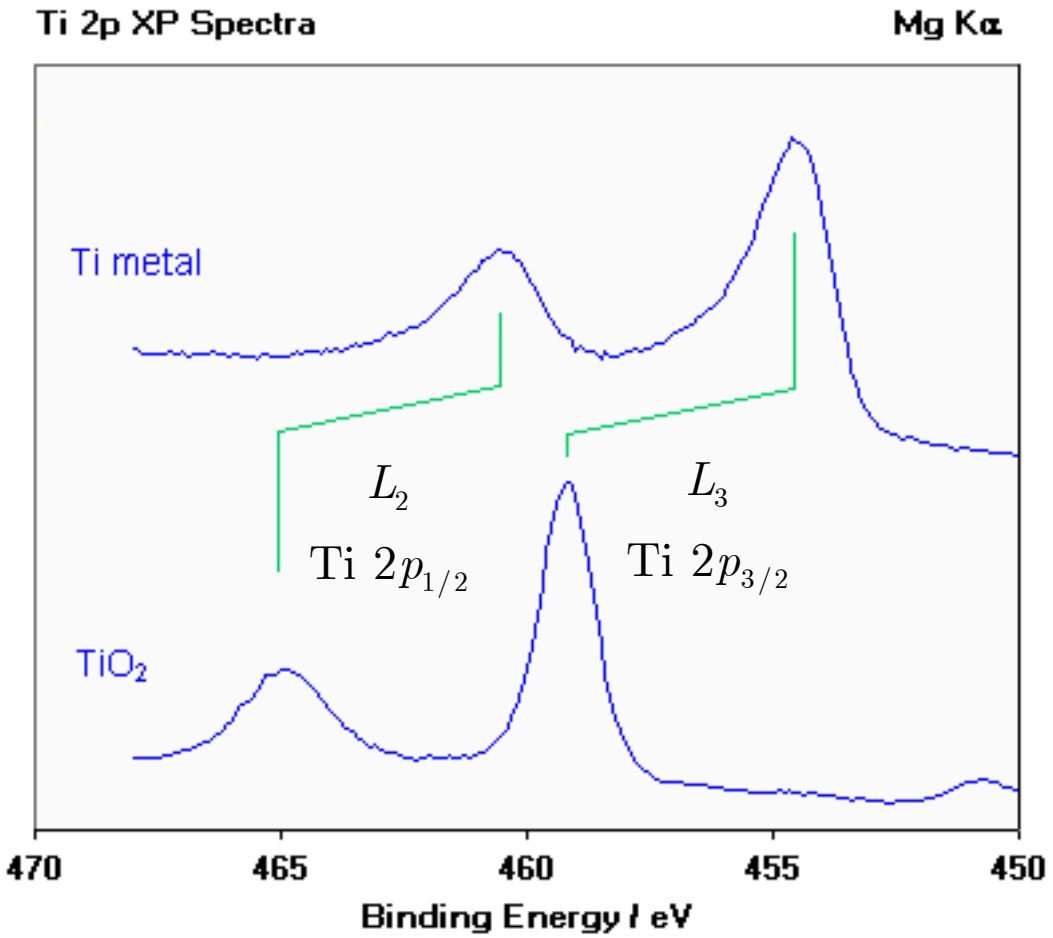

notice orientation of energy scale

3.2.1 X-ray Photoelectron Spectroscopy (XPS)

$4f_{7/2}$

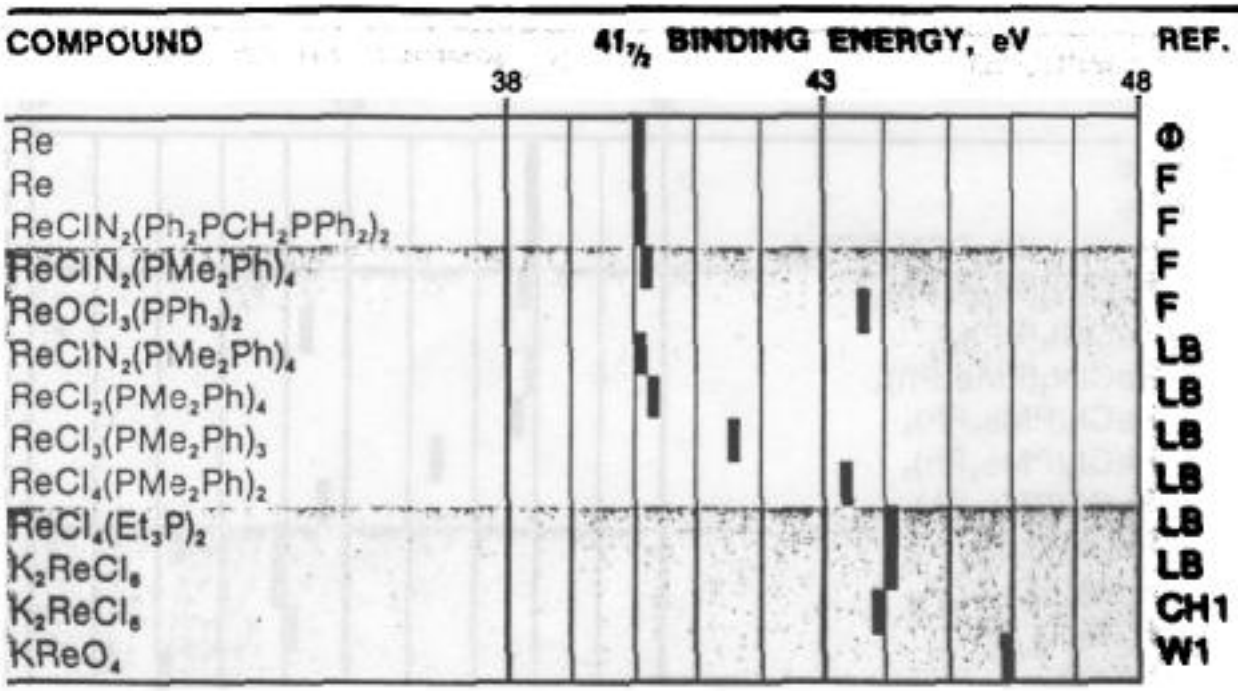

$\mathrm{Re}(0) \rightarrow$

$\mathrm{Re}(VII) \rightarrow$

Satellite Features in Core Level PES Spectra

- Additional features are often observed in a PES spectrum
- atomic orbital picture is simplistic – two sources of complication
  - atomic multiplets (states not orbitals)
  - charge transfer effects (molecules not atoms)
- Ground State Atomic Term Symbols (*a.k.a.* atomic multiplets)

$$3d^1 \rightarrow {}^2D$$
$$3d^2 \rightarrow {}^3F, {}^1G, {}^3P, {}^1D, {}^1S, \ldots$$
$$3d^5 \rightarrow {}^4S, {}^4G, {}^4P, {}^4D, {}^2I, {}^4F, {}^2D, {}^2F, \ldots$$

  - excited state terms are even more complicated
  - coupling of core hole with valence electrons (*e.g.* $2p^5 3d^n$)

Atomic Multiplets in XPS Spectra

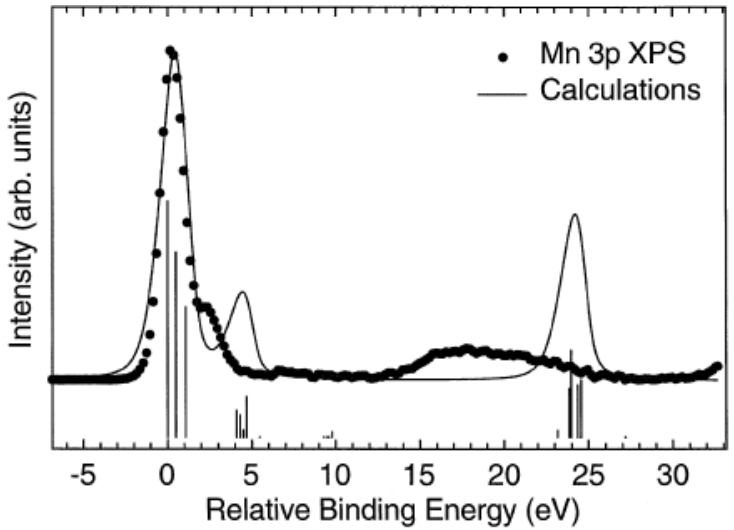

FIG. 1. Theoretical and experimental $3p$ level XPS spectra; experimental data for MnO taken from Ref. [16]. The vertical lines indicate the calculated E_{rel} and I_{rel}.

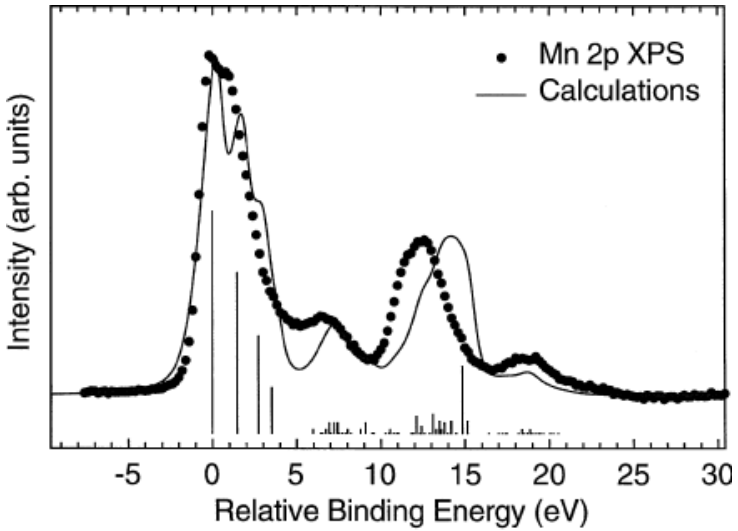

FIG. 2. $2p$ level XPS spectra; see caption for Fig. 1.

- can dramatically complicate the spectrum
- largest effect when purely *atomic* spectra…
  - remember: multiplet effects come from electron-electron repulsion
  - repulsion decreases with electron delocalisation (covalency of metal-ligand bonds)

Effects of Metal-Ligand Covalency in XPS Spectra

- delocalization over ligands complicates GS and ES wavefunctions
- decreases effect of atomic multiplets (collapses multiplets)
- adds "charge transfer" terms to the wavefunctions
  - delocalization onto ligands is included by adding additional term

$$\psi_g^{atomic} = \left|2p^6 3d^n\right\rangle$$

$$\psi_g^{CT} = \alpha\left|2p^6 3d^n\right\rangle \pm \sqrt{1-\alpha^2}\left|2p^6 3d^{n+1}\underline{L}\right\rangle$$

$$\psi_e^{CT} = \alpha\left|2p^5 3d^n\right\rangle \pm \sqrt{1-\alpha^2}\left|2p^5 3d^{n+1}\underline{L}\right\rangle$$

- additional states for transitions to occur…
  - formally forbidden (two-electron)
  - can only occur if *electronic relaxation* occurs
    - change in wavefunction upon ionisation

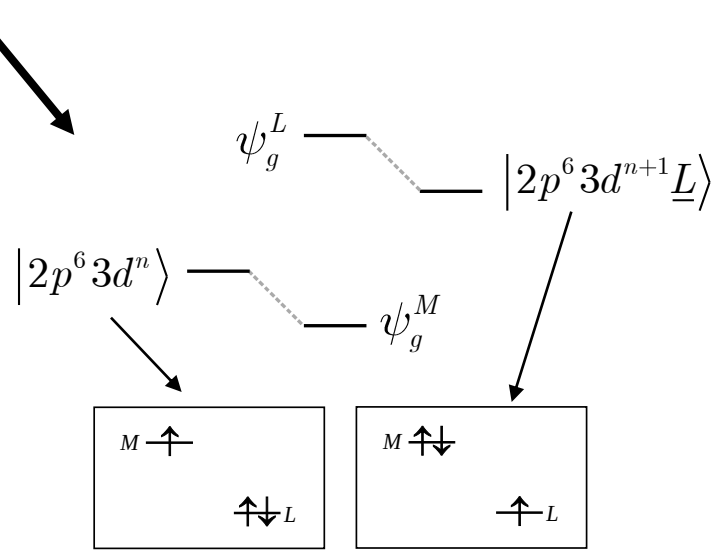

3.2.1 X-ray Photoelectron Spectroscopy (XPS)

- Core Fe $2p_{3/2}$ spectrum of $[FeX_4]^{2-,1-}$ complexes

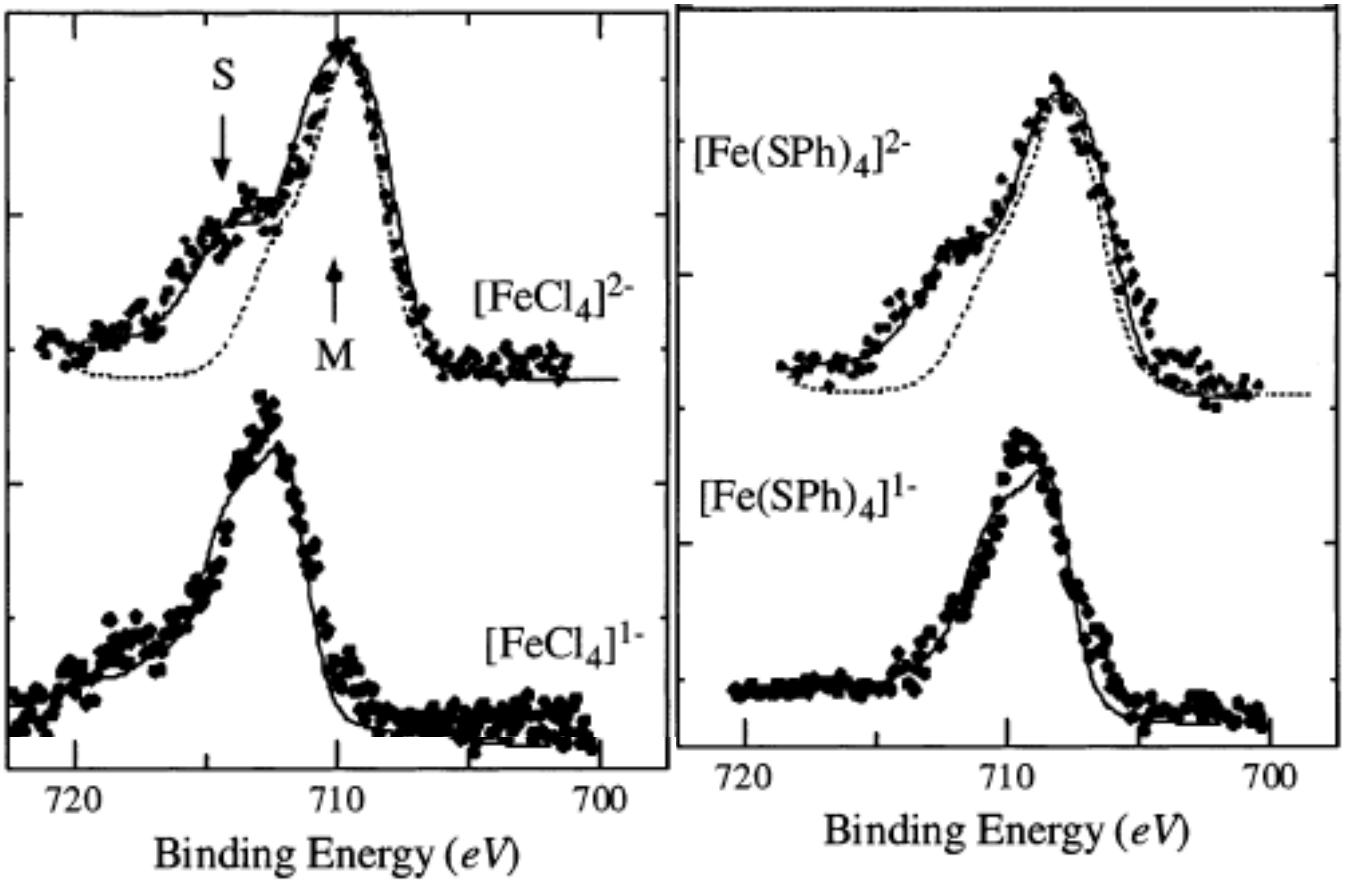

Auger Emission Spectroscopy

- E_k of emitted Auger electron is defined by:
- true for both Auger and Coster-Kronig
- independent of initial photoionisation
  - can use fixed frequency X-ray tubes
  - can also use electron gun (most common)
- AES is not very sensitive to environme
  - mostly effective for surface elemental anal
  - but will always show up in PES spectra!

$$E_k = E_1 - E_2 - E_3$$
$$= \Delta E_{12} - E_b$$

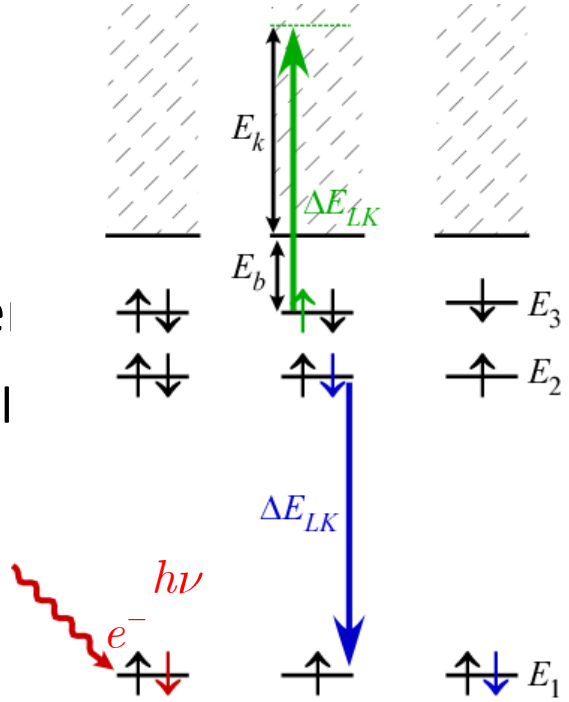

X-ray Absorption Spectroscopy

- Comparison with PES
  - lots of differences
  - somewhat analogous but different…

	PES	***XAS***
scan	E_k	$h\nu$
detect	primary e^-	$h\nu$, all e^-
result	peaks	edges (+ peaks)

- three distinct regions defined in relation to ionisation energy:
  - pre-edge
  - edge jump | (XANES)
  - post-edge (EXAFS)

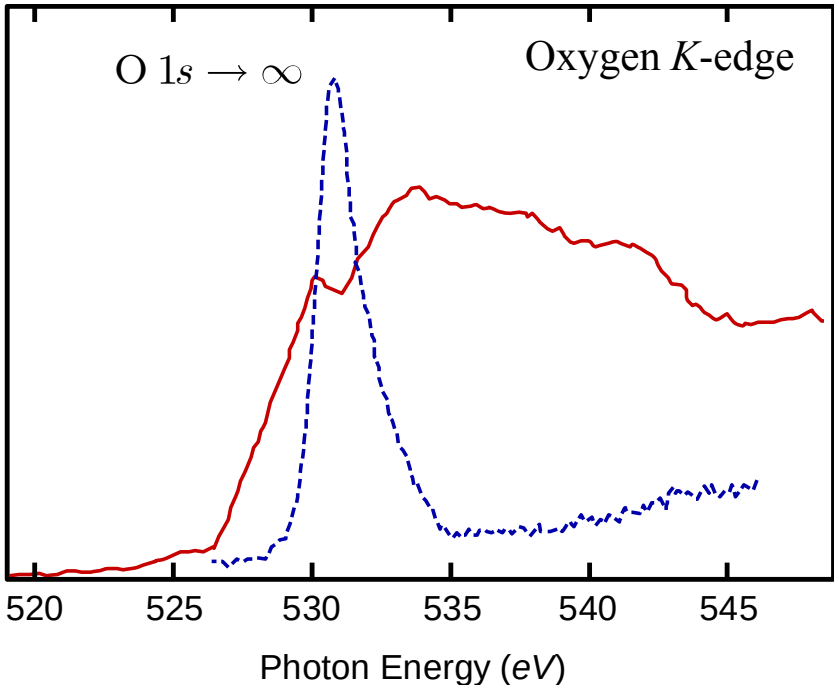

Regions of the XAS Spectrum

- The edge and pre-edge regions
  - generally known as X-ray Absorption Near Edge Structure (XANES)
  - region that occurs at or near the ionisation peak
  - bound state transitions (not complete ionisations!)
    - transitions handled in same way as Abs (except electron taken from core orbitals)
  - yields information about *electronic structure*

- The post-edge region
  - Extended X-ray Absorption Fine Structure (EXAFS)
  - oscillatory structure *after* ionization peak
  - results from *scattering* of photoelectrons with the surrounding atoms
  - yields *geometric structure* information

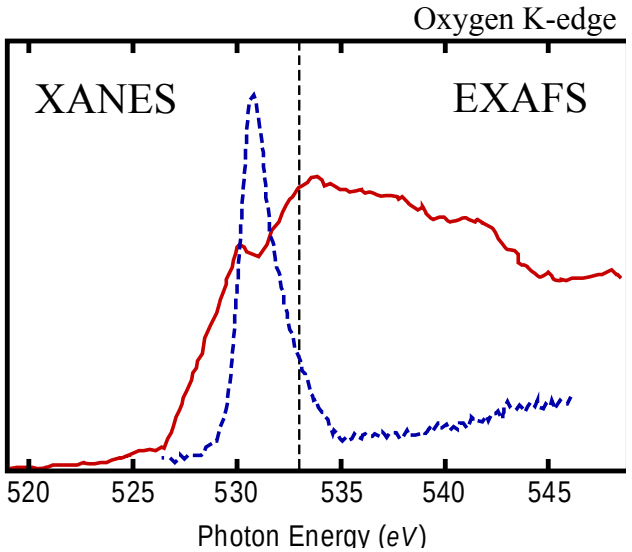

Scattering of Photoelectrons

- photoemission from an isolated atom:
  - ionisation edge jump
  - decay as you get away from resonance
- photoemission from an atom within a specific arrangement of other atoms:
  - additional regular oscillations
  - scattering from other atoms
- interference effect on photoabsorption causes by neighbouring atoms:
  - like diffraction
  - use scattering theory to get geometric inform

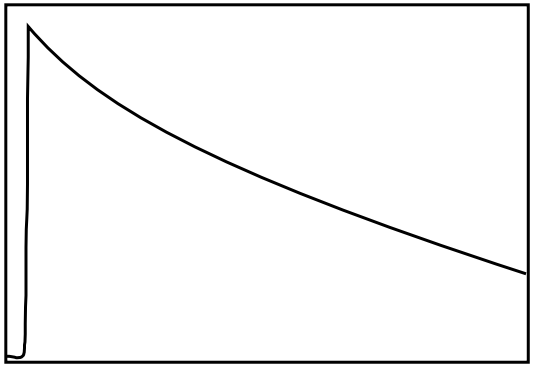

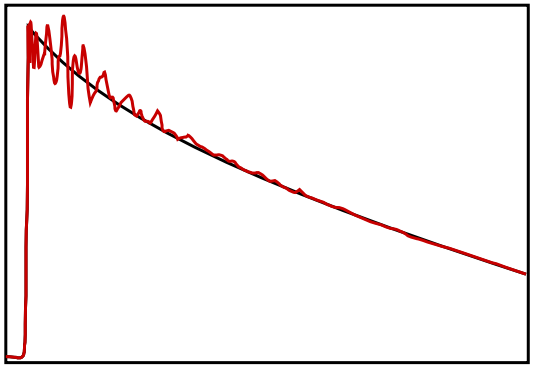

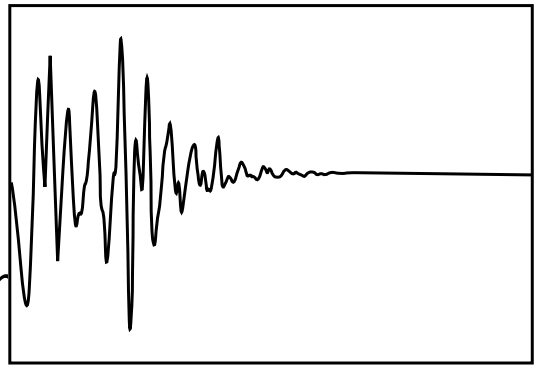

Obtaining XAS data

- measure the absorption of X-rays at different photon energies
- Three basic ways to measure absorption:
  - X-ray Transmission
    - direct measurement like UV/Vis Abs experiments
  - Total Fluorescence Yield (TFY) $I\ E\ \propto \sigma_{h\nu}\ E$
    - indirect measure – assumes
  - Total Electron Yield (TEY) $I\ E\ \propto \sigma_{Auger}\ E$
    - indirect measure - assumes

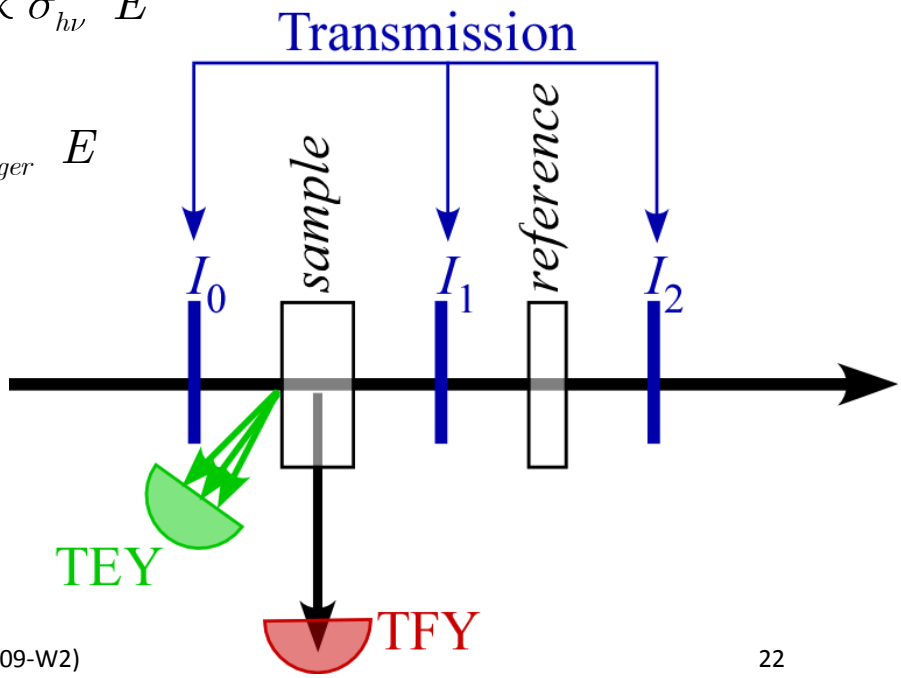

3.2.2 X-ray Absorption Spectroscopy (XAS)

X-ray Diffraction (XRD)

- X-ray scattering
  - interaction with electrons
  - large penetration depth
- external directional source
  - requires long-range order
  - sees all scatterers
- biggest problem
  - phase of scattering
  - use MAD/heavy atom replacement

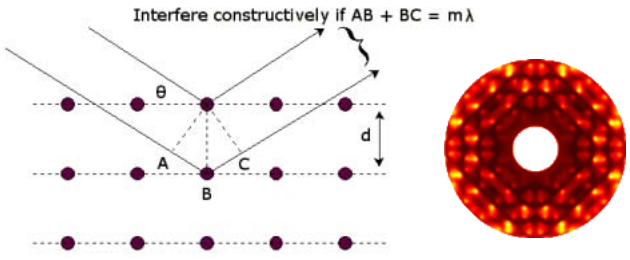

EXAFS

- electron scattering
  - interaction with electronic potential
  - short penetration depth
- localized internal source
  - sees short-range order
  - only sees nearby scatterers
- biggest problem
  - phase of scattering
  - use references/*ab initio* calcs

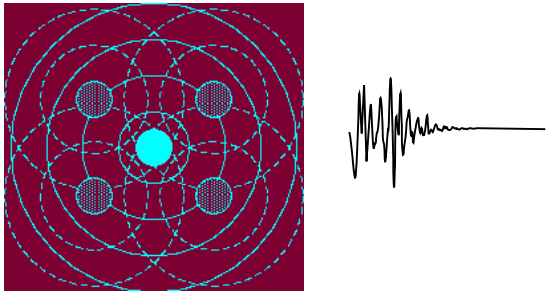

Basic Theory of EXAFS

- oscillations are visualized as $\chi(k)$

$$\chi(E) = \frac{\mu(E) - \mu_0(E)}{\mu_0(E)}$$

- *k* relates to photoelectron wavefunction
  - known as wave vector $k = \sqrt{2m_e\hbar^2 \ E - E_0}$
  - easily convert *E* to *k* $k \propto \sqrt{\Delta E}$

Note: doubling the *E* range gives ~40% more *k*-range

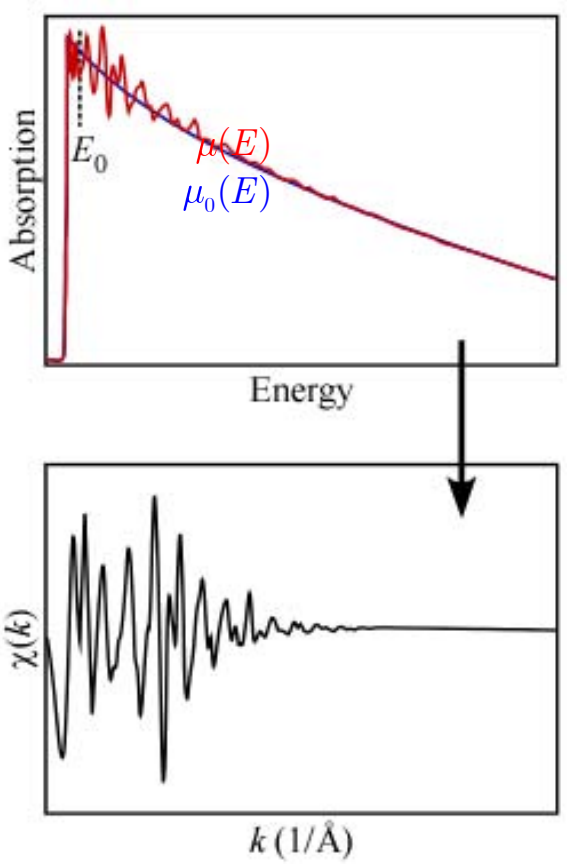

notice units of *k* space…

- more data means more periods of oscillation
  - getting higher *k* data is very useful (not always feasible)

    e.g. *k*-range of 0-12 is good, but 0-15 is much better

The EXAFS Equation

- semi-classical derivation of electron scattering for *K*-shell EXAFS:

$$\chi(k) = -S_0^2 \sum_i N_i \frac{\left| f\ \pi, k \right|}{kR_i^2} e^{-2\sigma_i^2 k^2} e^{-2R_i/\lambda\ k} \sin\ 2kR_i + 2\delta_1 + \varphi_i\ \pi, k$$

$S_0^2 \equiv$ amplitude reduction factor (due to electronic relaxation)

$N_i \equiv$ number of scattering atoms of a particular type

$e^{-2R_i/\lambda\ k} \equiv$ damping factor to account for electron mean free path (λ)

$R_i \equiv$ distance to atom i

$e^{-2\sigma_i^2 k^2} \equiv$ Debye-Waller factor (accounts for disorder in the sample)

$f\ (\pi, k) \equiv$ scattering amplitude of atom i

$\delta_1 \equiv$ phase shift of the photoelectron due to photoemitting atom

$\varphi_i\ (\pi, k) \equiv$ phase shift of the photoelectron due to scattering atom

Contributions to EXAFS oscillations

- the EXAFS is effectively *a sum of sinusoidal waves* that are affected by
  - the number of nearby scatterers (grouped by "geometric equivalence")
    - amplitude
  - the identity of the scatterers
    - phase
    - amplitude
  - the distance of the scatterers from the photoemitting atom
    - period of the wave
    - damping of amplitude
  - the disorder (both static and dynamic) of the scatterers
    - damping of amplitude

Fourier Transformation – moving to "real" space

- the *k*-space data can be transformed into *R*-space through FT:

$$FT(\chi(k)) = \mathrm{Re}\ \chi(k) + i\,\mathrm{Im}\ \chi(k)$$

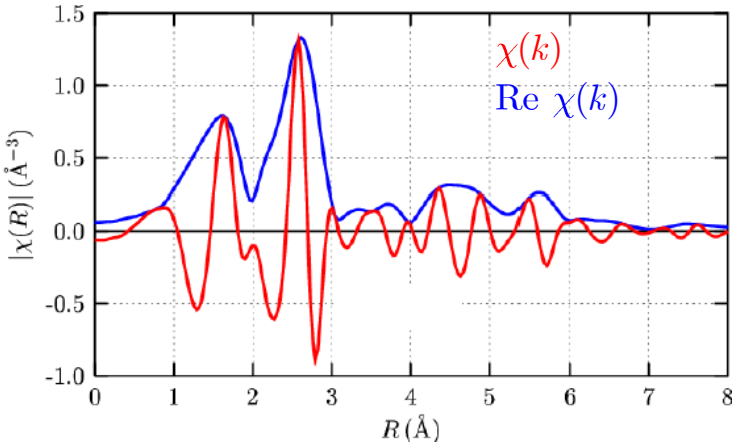

- each set of scatterers corresponds to a peak at a certain "distance"…
  - distance is NOT correct distance
  - distance has to be correctly for phase shift that occurs due to scatterers
  - phase shift is different for each type of atom!

$$\sin\ 2kR_i + 2\delta_1 + \varphi_i\ \ \pi, k$$

for n = 1 atoms (N, O):
shift is usually ~ **-0.5Å**

3.2.2 X-ray Absorption Spectroscopy (XAS)

Number of Scatterers

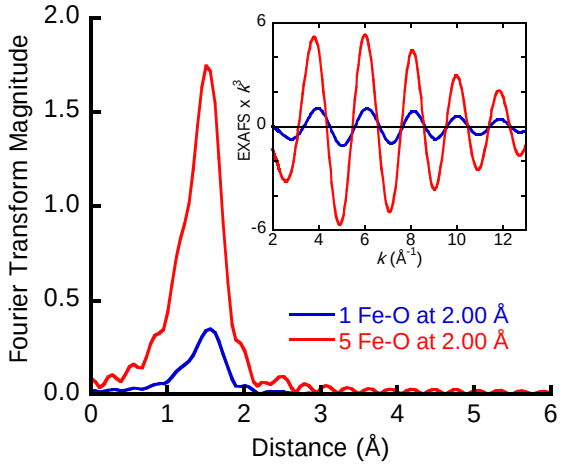

Identity of Scatterers

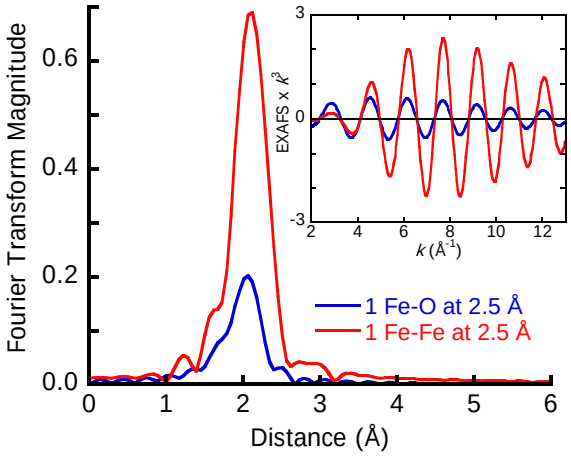

Distance from Photoemitter

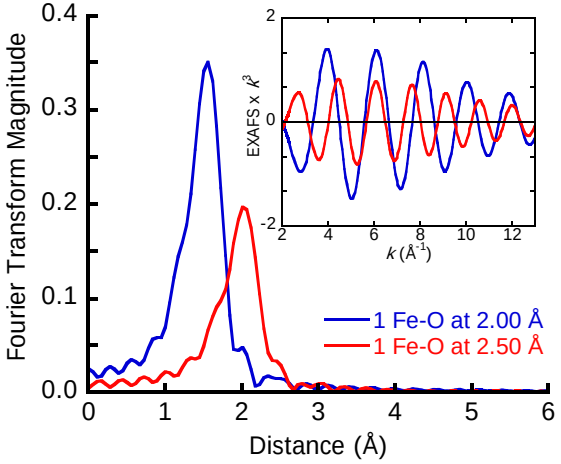

Amount of disorder

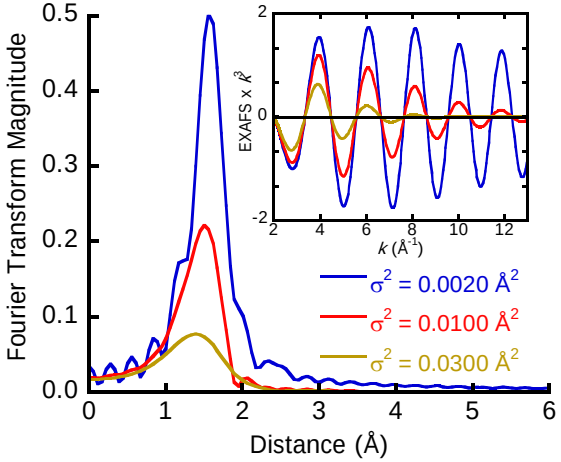

Multiple Scattering Pathways

- scattering is not necessarily a single event…
- can also have more complex scattering paths
  - to/from the same atoms
  - connecting three or more atoms
- phase shifts for multiple scattering paths is more complex
- depends on angle between scatterers
  - 180° creates constructive interference
  - 90° creates destructive interference

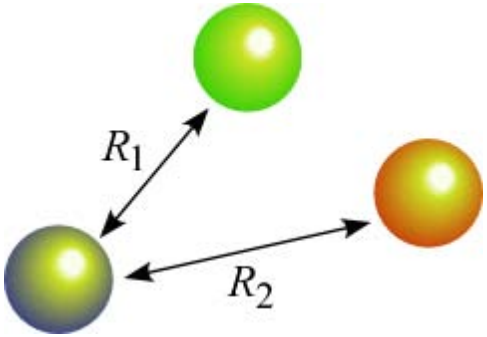

single scattering

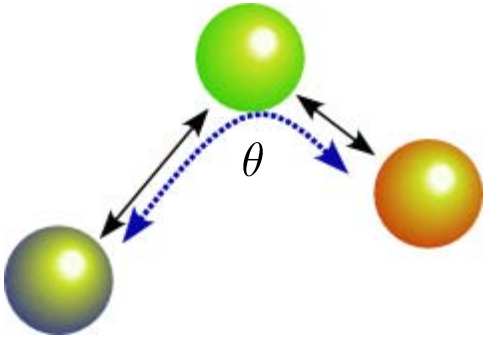

multiple scattering

General Approach to Fitting EXAFS Data

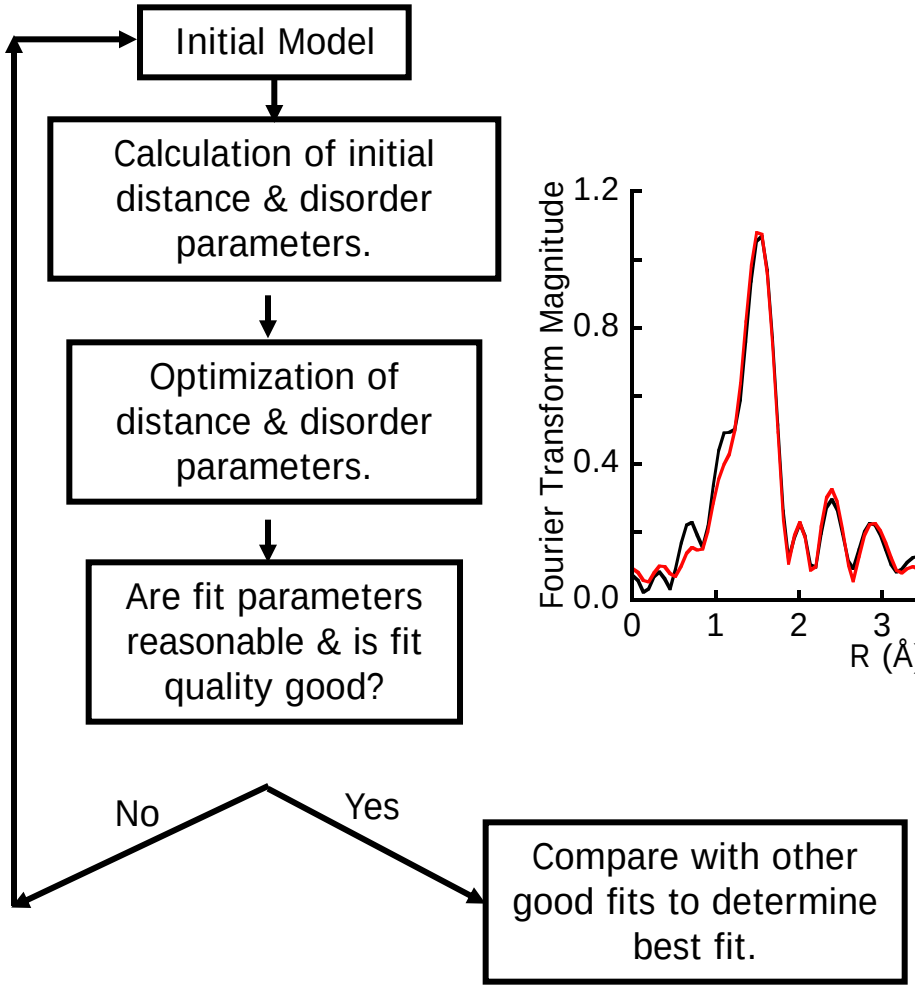

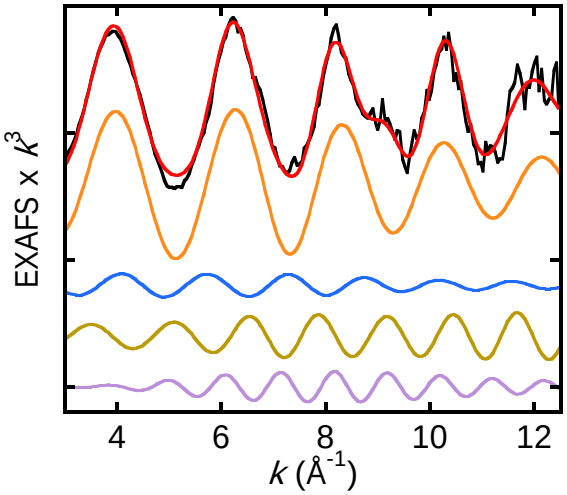

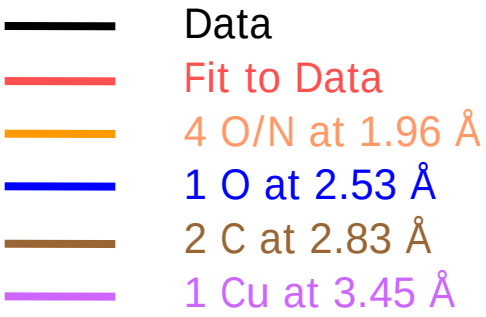

3.2.2 X-ray Absorption Spectroscopy (XAS)

- *e.g.* EXAFS deconvolution – Nature of Cu catalyst on ZnO surface

  - heterogeneous catalytic system for methanol synthesis

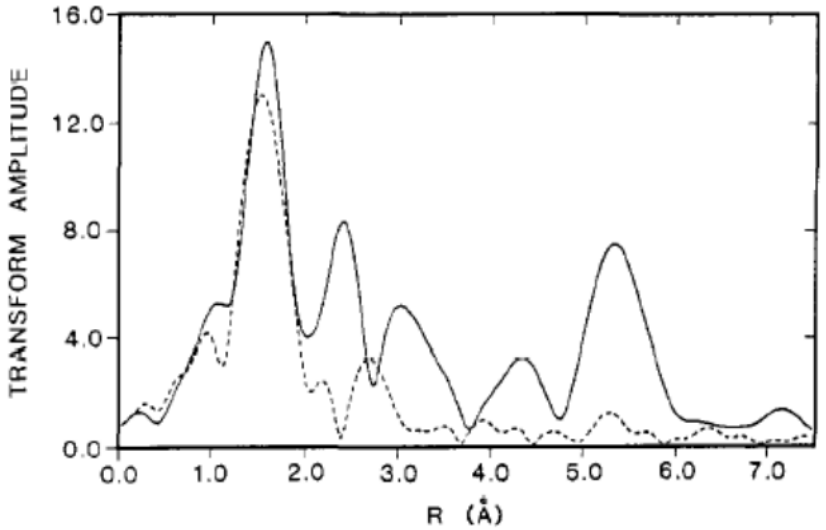

Figure 4. Fourier transforms of the EXAFS data over $k = 3.3–12.3$ Å^{-1} for the calcined 5% Cu/ZnO sample at room temperature (dash) and at 77 K (solid).

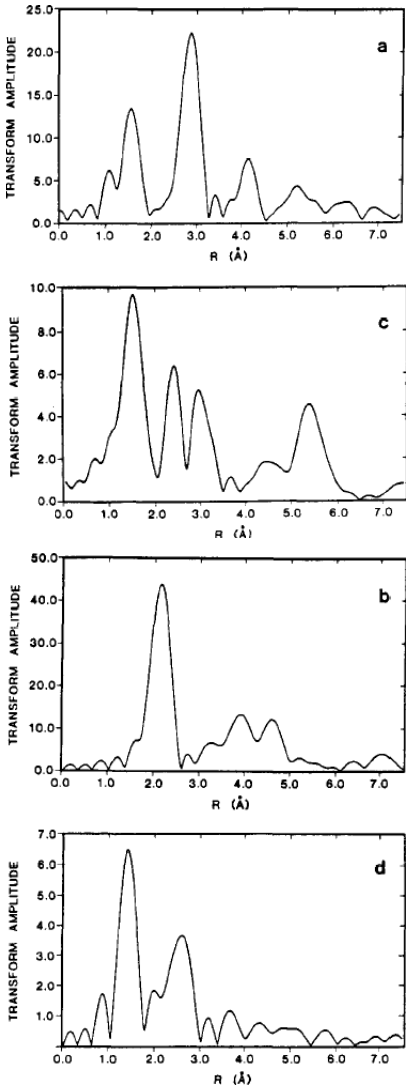

3.2.2 X-ray Absorption Spectroscopy (XAS)

- *e.g.* EXAFS deconvolution – protocathechuate dioxygenase

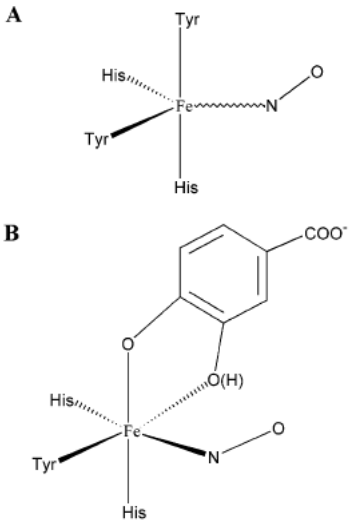

Figure 5. Spectroscopically effective structures for (A) $Fe^{III}PCD\{NO^-\}$ and (B) $Fe^{III}PCD\{PCA,NO^-\}$. The catecholate can either be the monoanion or the dianion depending on the pK_a at the $Fe^{III}-NO^-$ site.

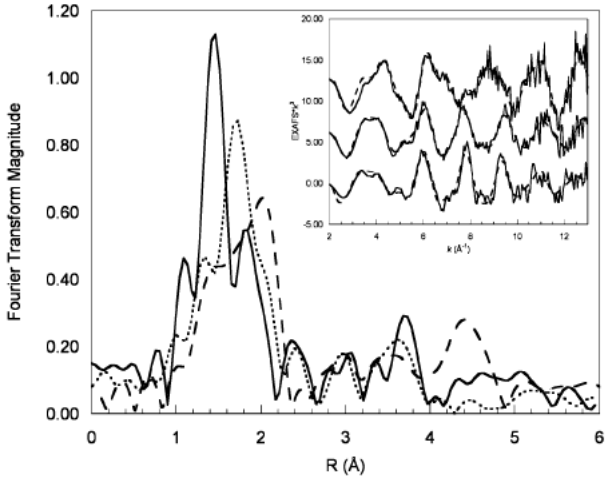

Figure 2. (a) Fourier transform of data for $Fe^{III}PCD\{\}$ (—), $Fe^{III}PCD\{NO^-\}$ (•••), and $Fe^{III}PCD\{PCA,NO^-\}$ (- - -). Inset: EXAFS data (—) and fits to the data (- - -) of $Fe^{III}PCD\{\}$ (top), $Fe^{III}PCD\{NO^-\}$ (middle), and $Fe^{III}PCD\{PCA,NO^-\}$ (bottom). Data for $Fe^{III}PCD\{\}$ and $Fe^{III}PCD\{NO^-\}$ have been offset by 12 and 6 units, respectively.

Table 2. EXAFS Fit Results for $Fe^{III}PCD\{\}$, $Fe^{III}PCD\{NO^-\}$, and $Fe^{III}PCD\{PCA,NO^-\}$

	$Fe^{III}PCD\{\}$			$Fe^{III}PCD\{NO^-\}$			$Fe^{III}PCD\{PCA,NO^-\}$		
	CN	R (Å)	σ^2 (Å^2)	CN	R (Å)	σ^2 (Å^2)	CN	R (Å)	σ^2 (Å^2)
Fe−N/O	3	1.88	0.00220	1	1.91	0.00323	1	1.93	.00288
Fe−N/O	2	2.10	0.00114	4	2.11	0.00276	3	2.10	0.00328
Fe−N/O							2	2.44	0.00173
Fe−C/N SS[a]	4	3.01	0.00702	4	3.00	0.01008	4	2.82	0.00989
Fe−C MS[a]	6	3.33	0.00104	6	3.24	0.00705	7	3.39	0.00317
Fe−C MS	6	4.30	0.00737	6	4.33	0.00655	8	4.31	0.00800
avg. Fe−N/O R (Å)		1.97			2.07			2.19	
error[b]		0.91			0.40			0.50	

[a] SS: single scattering. MS: multiple scattering. [b] Error is defined as $F = \sum[(\chi_{exp} - \chi_{obsd})^2 k^6]/\sum[\chi^2_{exp} k^6]$.

Issues to remember with EXAFS

- unique approach to get geometry in non-crystalline samples
- standard approach to data acquisition gives AVERAGE spectrum
  - contributions from multiple sites can be difficult to deconvolute
- there are LOTS of parameters
  - too many to give unique fit
  - get chemically reasonable fit based on information from other sources
  - use *ab initio* simulations to compare to data
- Sensitivity of data differs for different parameters:
  - very sensitive to bond distances (R_i error within 0.02Å)
  - very *insensitive* to coordination number (N_i is usually within +/- 1)

3.2.2 X-ray Absorption Spectroscopy (XAS)

X-ray Spectroscopic transitions

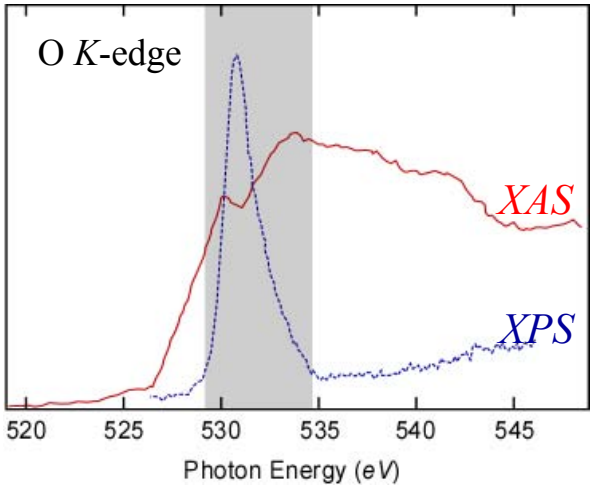

- ionisation edge - characterised by jump in intensity with slow decay
- transitions to bound states - discrete transitions to empty molecular orbitals
- also: transitions to Rydberg states
  - final state is similar to ionisation but electron is not actually removed
- intense transitions will be electric dipole allowed such that:

$$\left\langle \Psi_g \left| \hat{r} \right| \Psi_e \right\rangle \neq 0$$

$$\begin{vmatrix} \Delta S = 0 \\ \Delta l = \pm 1 \\ g \rightarrow u \end{vmatrix}$$

- for *K*-edge (1*s*) XAS, we can expect
  - edge jump for ionisation
  - strong transitions to valence orbitals that contain n*p* character
- *Important*: transitions rely on overlap between initial and final states
  - 1*s* orbital is very localized - transitions will be localized on absorber atom…

Metal K-edge XANES Analysis

- Simplest example: Zn^{II} ($3d^{10}$) O_h system
  - Zn 3*d* orbitals are full
  - lowest energy bound state transitions are 1*s*→4*p* (4*s* are also empty but *s*→*s* not ED allowed)
  - look at atomic description of 1*s*→4*p* bound state transition:

$$\left|1s^2 2s^2 2p^6 3s^2 3p^6 3d^{10} 4s^0 4p^0\right\rangle \xrightarrow{h\nu} \left|1s^1 2s^2 2p^6 3s^2 3p^6 3d^{10} 4s^0 4p^1\right\rangle$$

$$\left|1s^2 4p^0\right\rangle \xrightarrow{h\nu} \left|1s^1 4p^1\right\rangle$$

Group Theory in O_h Symmetry

$${}^1A_{1g} \otimes {}^1A_{1g} = {}^1A_{1g} \xrightarrow{h\nu} {}^2A_{1g} \otimes {}^2T_{1u} = {}^1T_{1u} + {}^3T_{1u}$$

$${}^1A_{1g} \xrightarrow{h\nu} {}^1T_{1u}$$

spins coupling gives $S = 0, 1$
orbital part gives T_{1u}

$$\vec{\mu}_{x,y,z} \mapsto (\vec{x}, \vec{y}, \vec{z}) \mapsto t_{1u}$$

- 4*p* orbital is very diffuse – will have strong overlap with ligand orbitals…
  - get distribution of 1*s*→4*p* intensity to charge transfer (CT) peaks [remember PES!]
  - ligand interactions must have t_{2g} symmetry (GT allowed mixing with 4*p* orbitals in O_h)

Zn K-edge XANES

- contributions to 1*s*→4*p* are basicall
  at the 1*s* ionisation edge jump
- symmetry & nature of ligands changes effect of CT states

$$\Psi_f = \alpha\left|1s^1 4p^1 L\right\rangle + \sqrt{1-\alpha^2}\left|1s^1 4p^2 \underline{L}\right\rangle$$

- not particularly informative
  - somewhat sensitive to symmetry
  - differences are relatively small

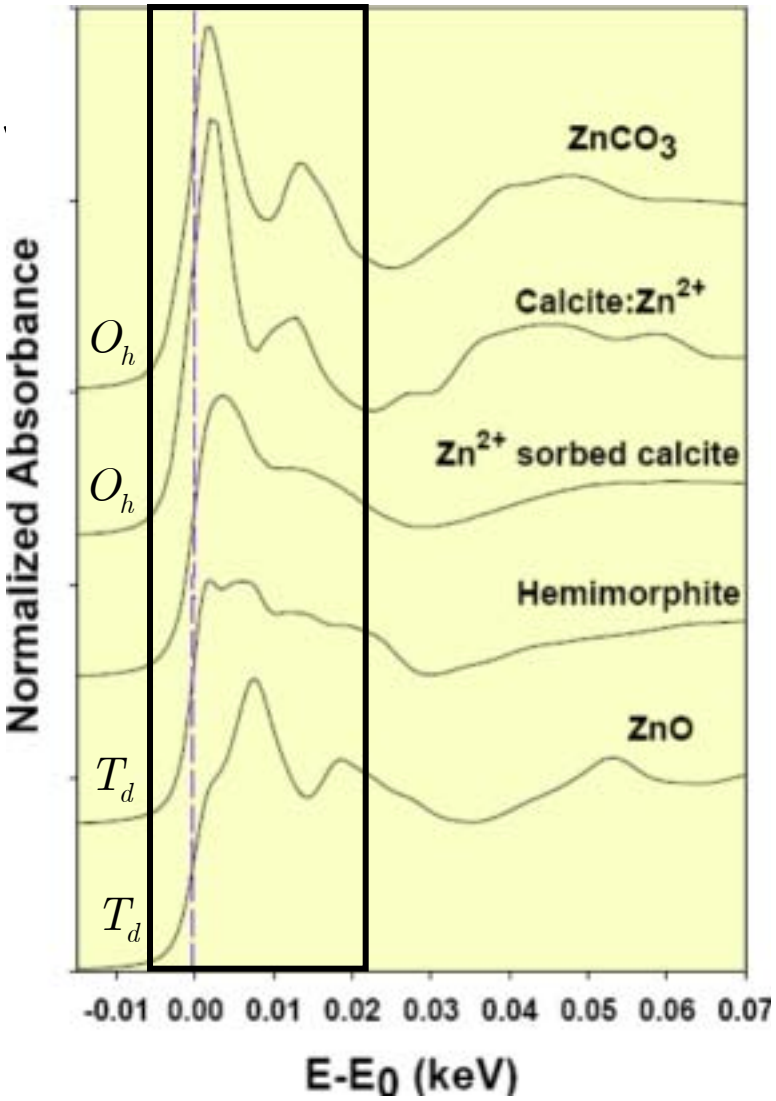

Cu K-edge XANES Analysis

- Cu^{I} is basically the same as $Zn^{II} \rightarrow 3d^{10}$
  - Cu 3*d* orbitals are full
  - 1*s* → 4*p* + CT contributions at/near the 1*s* edge jump
  - 4*p* splitting and CT contributions provide reference points for specific geometries / coordination numbers
- Cu^{II} K-edge XANES is more interesting…
  - edge jump should be at different energy (ΔZ_{eff})
  - still have Cu 1*s*→4*p*
  - Cu $3d^9$ system – hole in 3*d* manifold, but...

$$\left|1s^2 3d^9 4p^0\right\rangle \rightarrow \left|1s^1 3d^9 4p^1\right\rangle \text{ is electric dipole allowed}$$

$$\left|1s^2 3d^9 4p^0\right\rangle \rightarrow \left|1s^1 3d^{10} 4p^0\right\rangle \text{ is electric dipole forbidden}$$

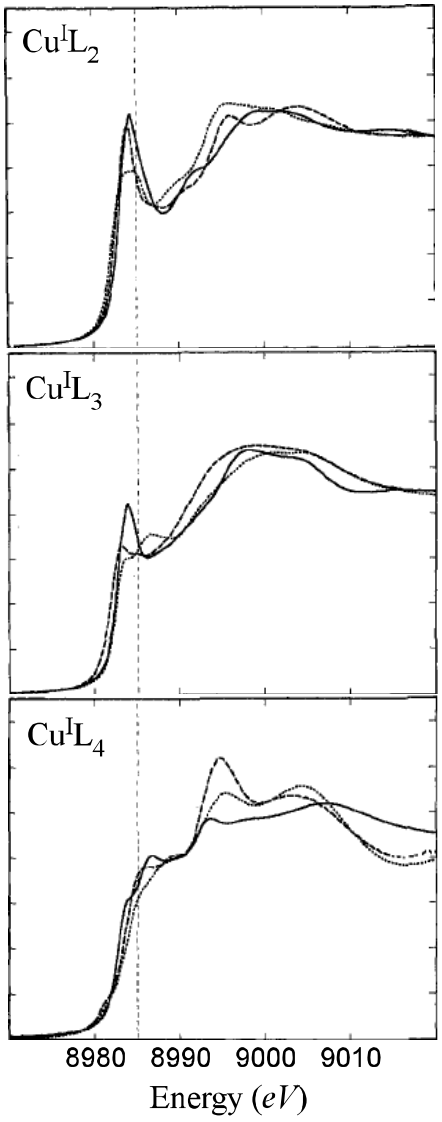

Cu^{II} K-edge XANES Analysis

- XANES spectra are very different
  - edge jump is at higher energy in Cu^{II} since Cu 1*s* is at deeper binding energy

$$E_{ionisation}^{Cu^{II}} > E_{ionisation}^{Cu^{I}}$$
$$Z_{eff}^{Cu^{II}} > Z_{eff}^{Cu^{I}}$$

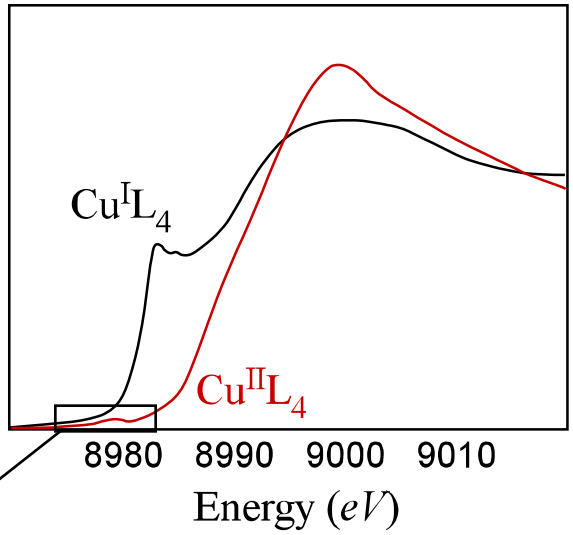

- if you look carefully, a very weak peak is observable in the pre-edge region…

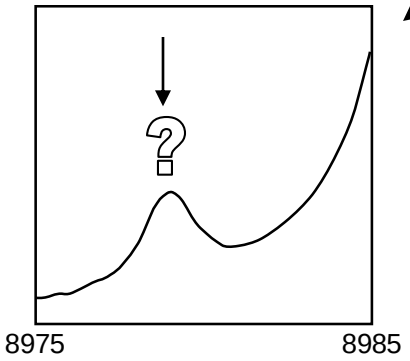

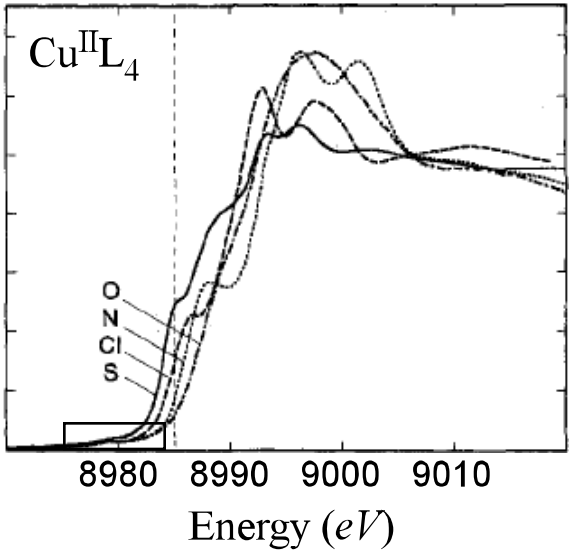

Pre-edge features in Metal K-edge XAS Spectra

- peaks are generally very weak
- result from 1*s*→3*d* transitions: $\left|1s^2 3d^n\right\rangle \rightarrow \left|1s^1 3d^{n+1}\right\rangle$
- possible final states can be decomposed into two terms
  - *e.g.,* in O_h symmetry

$$\left|\begin{array}{l} 1s^1 \rightarrow {}^1A_{1g} \\ 3d^{n+1} \rightarrow {}^{2S+1}\Gamma \end{array}\right.$$

will affect spin but not symmetry of final states

$${}^{2S+1}\Gamma \otimes {}^1A_{1g} = {}^{2S}\Gamma + {}^{2S+2}\Gamma$$

easily solved through Ligand Field Theory:
Tanabe-Sugano Matrices

- therefore, can use d^{n+1} Tanabe Sugano diagrams
- but why can we see these transitions?
  - 1*s*→3*d* transitions are *electric quadrupole allowed*
  - proven by angle-dependence of peak intensities in Cu^{II} system →

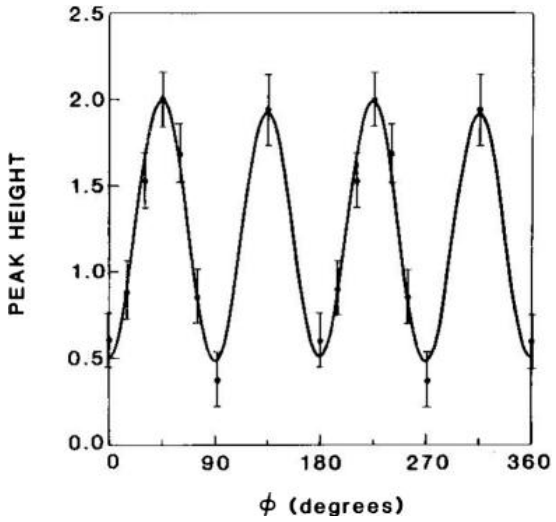

3.2.2 X-ray Absorption Spectroscopy (XAS)

- *e.g.* analysis of pre-edge features for O_h Fe^{II} Complexes
  - start with low-spin ferrous complexes
    - look for spin-allowed one-electron transitions

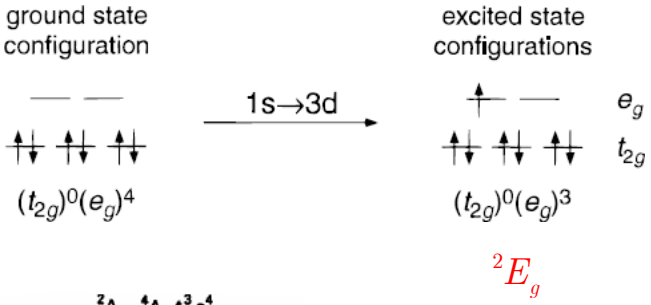

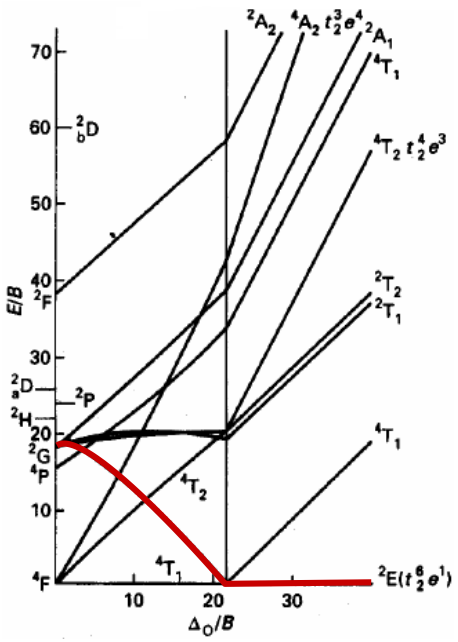

all other LF states
are from forbidden
two-electron transitions

no other ^2E to mix with so there should only be one pre-edge peak…

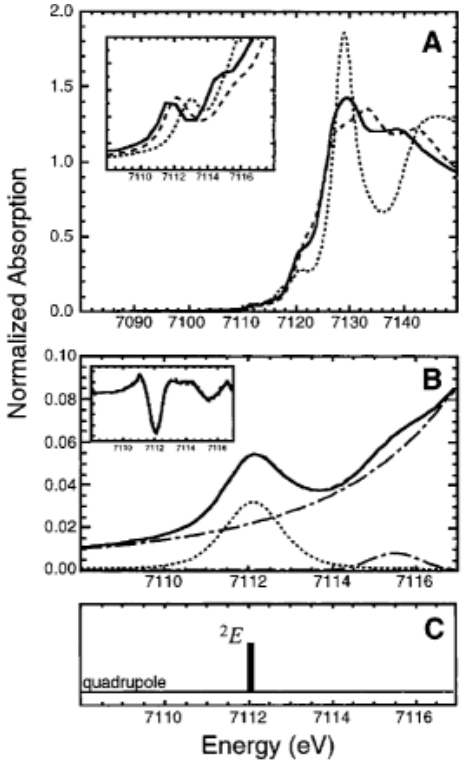

Figure 8. Fe K-edge XAS spectra, pre-edge fits, and theoretical analysis of octahedral low-spin Fe^{II} complexes. (A) Fe K-edge spectra of $Fe(HB(pz)_3)_2$ (—), $Fe(prpep)_2$ (- - -), and $K_4[Fe(CN)_6]\cdot 3H_2O$ (···) where the inset is an expansion of the 1s → 3d pre-edge region, with the normalized absorption scale being 0.0−0.1. (B) Fit to the Fe K-edge pre-edge region of $Fe(prpep)_2$ including the experimental data (—), a fit to the data (- - -), the background function (— -), and the individual pre-edge peak from the fit (···). An edge peak was also needed in the fit of this data and is shown (— -; see the text). The inset displays the second derivative of the data (—) and the second derivative of the fit to the data (- - -). (C) The single many-electron $d^{(n+1)}$ excited state.

3.2.2 X-ray Absorption Spectroscopy (XAS)

- what about high-spin ferrous complexes?
  - more complex…

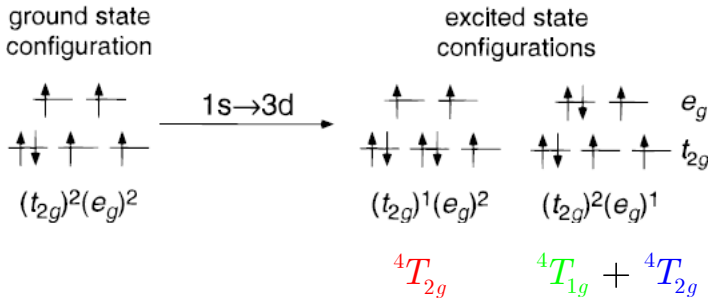

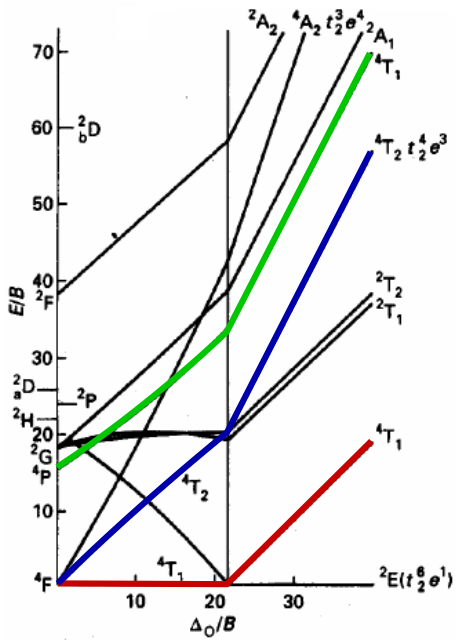

other LF states result from forbidden two-electron transitions

intensity of peaks will depend on covalency but it's not easy since peaks are so weak…

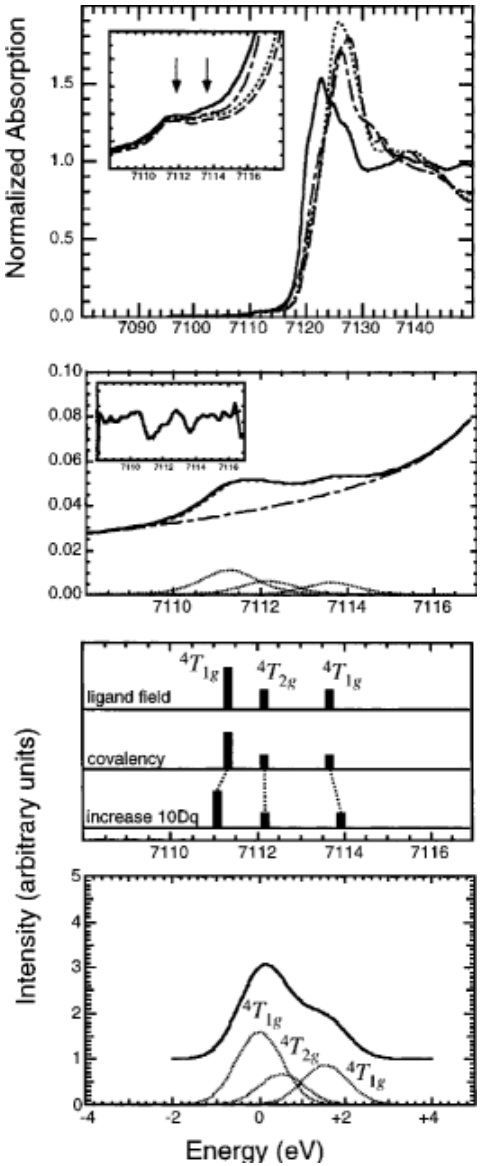

Effect of lower symmetry and "3d-4p mixing"

- 1*s*→3*d* are very weak because they are not ED allowed
- are there situations where this is not true?
  - if final states include some 4*p* character (even just a little)

remember: $\left\langle \Psi_g \left| \hat{r} \right| \Psi_e \right\rangle \gg \left\langle \Psi_g \left| \hat{r}^2 \right| \Psi_e \right\rangle$ by 2 orders of magnitude!

- how can we get 3*d*-4*p* mixing? (think back to *Abs*!)
  - centrosymmetric (*i.e.*, with inversion symmetry) cannot have 4*p* mixing

$$O_h \rightarrow \begin{matrix} 3d \equiv e_g + t_{2g} \\ 4p \equiv t_{1u} \end{matrix} \qquad D_{4h} \rightarrow \begin{matrix} 3d \equiv a_{1g} + b_{1g} + b_{2g} + e_g \\ 4p \equiv a_{2u} + e_u \end{matrix}$$

  - but non-centrosymmetric can…

$$T_d \rightarrow \begin{matrix} 3d \equiv e + t_2 \\ 4p \equiv t_2 \end{matrix} \qquad C_{4v} \rightarrow \begin{matrix} 3d \equiv a_1 + b_1 + b_2 + e \\ 4p \equiv a_1 + e \end{matrix}$$

3.2.2 X-ray Absorption Spectroscopy (XAS)

- Effect of C_{4v} distortions in ferrous complexes…

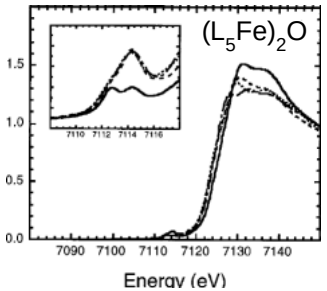

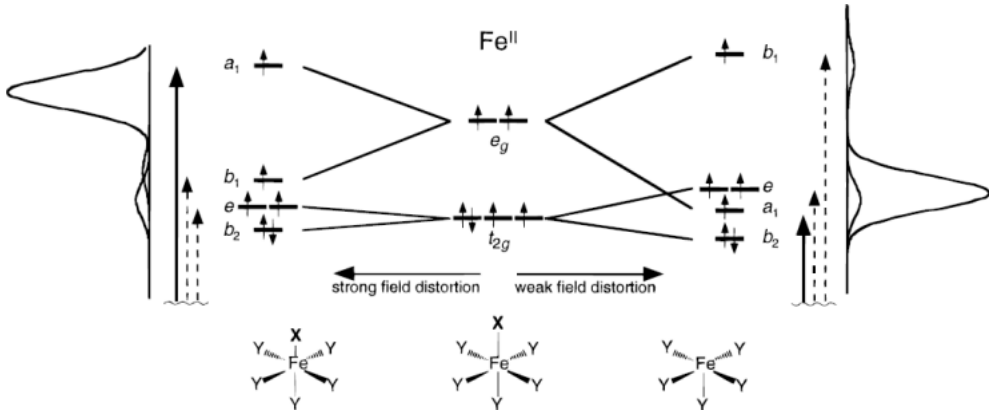

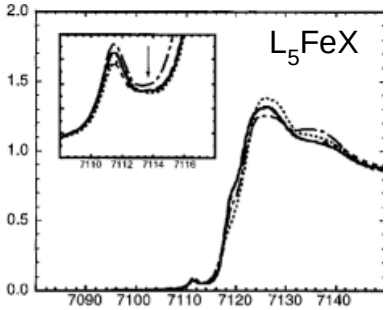

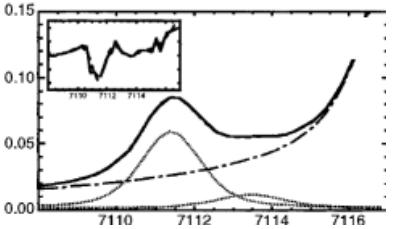

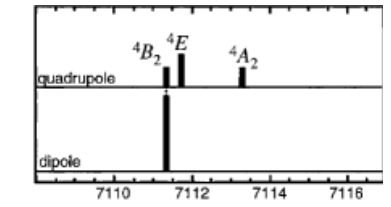

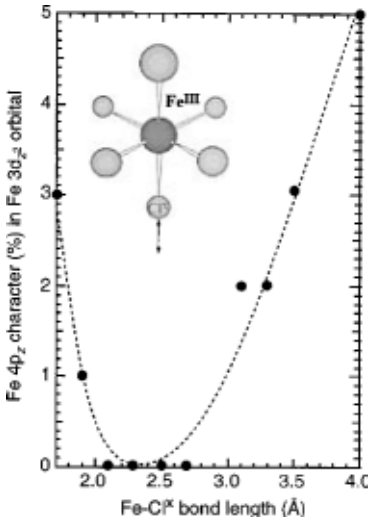

***distortion from O_h along z-axis causes*:**

splitting of final states
$4p$ mixing into $3d_{z^2}$ orbital

can be used to track distortions in metal active sites

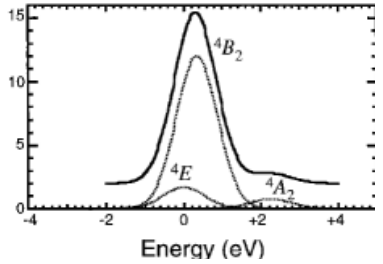

Summary of Metal K-edge XANES

- energy of edge jump is related to oxidation state (Z_{eff})
- 1*s*→3*d* transitions are very weak unless 4*p* mixing can occur
  - can use intensity and splitting to investigate ligand field surrounding metal
- 1*s*→4*p* transitions are very strong but masked by the edge jump (difficult to interpret)
- can be very useful in determining coordination number of metal complexes
  - good complement to EXAFS!
- biggest problems
  - intensity of pre-edge features is very weak (EQ mechanism)
  - edge jump is huge compared to electronic transitions
- solution – use metal *L*-edges (M 2*p* ionisation) instead of *K*-edges…
  - 2p→3d transitions are electric dipole allowed
  - edge jump is much weaker

Metal L-edge XANES

- biggest problem – final state analysis is more complicated
  - metal 2*p* hole is no longer *benign* $\left|2p^6 3d^n\right\rangle \rightarrow \left|2p^5 3d^{n+1}\right\rangle$
  - must include both spin and orbital coupling to $3d^{n+1}$
  - spin-orbit coupling!
- simplest case *L*-edges for Cu^{II} ($3d^9$) complexes
  - intensity of the L-edge peaks is directly related to the amount of 3*d* character in the singly-occupied orbital…

$$\Psi_{SOMO} = \alpha\left|3d\right\rangle - \sqrt{1-\alpha^2}\left|L\right\rangle$$

$$I \propto \left|\left\langle \Psi_f \left|\hat{r}\right| \Psi_i \right\rangle\right|^2 = \left|\left\langle \Psi_{2p} \left|\hat{r}\right| \Psi_{SOMO} \right\rangle\right|^2 = \left|\left\langle \Psi_{2p} \left|\hat{r}\right| \alpha\Psi_{3d} \right\rangle\right|^2$$

$$I = \alpha^2 I_{2p\rightarrow 3d}$$

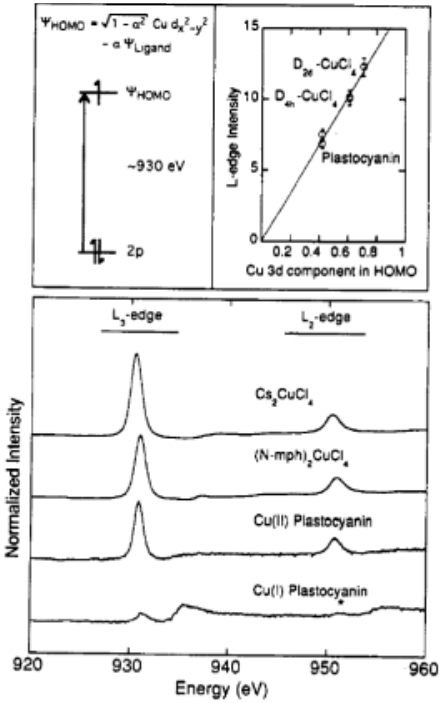

Figure 1. Intensity variation of Cu 2p to 3d Ψ_{HOMO} transition. Top left panel: Energy level diagram illustrating the observed Cu 2p to 3d Ψ_{HOMO} transition. Top right panel: Total integrated intensity of the L_2 and L_3 peaks normalized to the continuum intensity plotted as a function of estimated Cu $3d_{x^2-y^2}$ character in the HOMO; 5% error bars are included. Lower panel: Cu L-edge spectra of (from top to bottom) D_{2d}-Cs_2CuCl_4, D_{4h}-$(N\text{-mph})_2CuCl_4$, Cu(II) plastocyanin, and Cu(I) plastocyanin. The spectra have been normalized to the continuum intensity. Features marked with an asterisk (*) in the Cu(I) plastocyanin data arise from incomplete reduction.

K-edge XANES Spectra of non-metals

- for C, N, O – often called NEXAFS
- use similar approaches to understanding bound state transitions
- electric dipole allowed transitions dominate ($s \rightarrow p$)
  - good, because valence orbitals are often n*p* orbitals
    - C,N,O,F $\rightarrow$ 2*p*
    - P,S,Cl $\rightarrow$ 3*p*
- comparisons of free vs. bound ligands is often extremely informative
  - shifts in valence orbital energies
  - quantify charge donation into metal (*e.g.*, π-backbonding)
  - direct measure of covalency into metal
- gives alternative viewpoint to bonding
  - can see electronic structure from different perspectives
  - very useful since spectroscopy always perturbs system and each approach looks at things in a slightly different way

Summary of XANES Spectroscopy

- edge jump directly related to Z_{eff}
- effective probe of empty valence orbitals
  - electron delocalisation
  - covalency of species
  - energetic effect of bonding
- element specific
  - look directly at a particular component of a complex system
  - can often see system from several different perspectives